Lattice dynamics and thermal equation of state of platinum

Tao Sun,[1,*] Koichiro Umemoto,[2] Zhongqing Wu,[2] Jin-Cheng Zheng,[3] and Renata M. Wentzcovitch[2]
[1]*Department of Physics and Astronomy, Stony Brook University, Stony Brook, New York 11794, USA*
[2]*Department of Chemical Engineering and Materials Science, Minnesota Supercomputing Institute, University of Minnesota, Minneapolis, Minnesota 55455, USA*
[3]*Condensed Matter Physics & Materials Science Department, Brookhaven National Laboratory, Upton, New York 11973, USA*
(Received 22 January 2008; revised manuscript received 29 May 2008; published 28 July 2008)

Platinum is widely used as a pressure calibration standard. However, the established thermal equation of state (EOS) has uncertainties especially in the high *P*-*T* range. We use density-functional theory to calculate the thermal equation of state of platinum up to 550 GPa and 5000 K. The static lattice energy was computed by using the linearized augmented plane-wave method with local-density approximation (LDA), Perdew-Burke-Ernzerhof, and the recently proposed Wu-Cohen functional. The electronic thermal free energy was evaluated using the Mermin functional. The vibrational part was computed within the quasiharmonic approximation using density-functional perturbation theory and pseudopotentials. Special attention was paid to the influence of the electronic temperature on the phonon frequencies. We find that, in overall, LDA results agree best with the experiments. Based on the density-functional theory calculations and the established experimental data, we develop a consistent thermal EOS of platinum as a reference for pressure calibration.

DOI: 10.1103/PhysRevB.78.024304 PACS number(s): 71.15.Mb, 64.30.Ef, 05.70.Ce, 63.20.D−

I. INTRODUCTION

Platinum (Pt) is a widely used high-pressure standard. Its equation of state (EOS) at room temperature has been established by reducing shock Hugoniot[1–4] and by *ab initio* linear-muffin-tin-orbital (LMTO) calculations[4] up to 660 GPa. Mao *et al.*[5] used the EOS developed in Ref. 4 (Holmes *et al.*) to calibrate pressure in their compression experiment on Fe and Fe-Ni alloys. The bulk moduli measured at the earth's core pressure are substantially higher than those extrapolated from seismological observations.[6,7] A large pressure offset is needed to remove the discrepancy: about 8% at 100 GPa and 15% at 300 GPa. The origin of this offset is under investigation. One possibility is the EOS of Holmes *et al.* seriously overestimates pressure.[6] Singh[7] raised other possibilities. He noticed that the one-parameter EOS of platinum agrees with the EOS of Holmes *et al.* to 1% at high pressures and concluded that large systematic error in pressure scale is unlikely. He further proposed that the discrepancy due to the pressure on the sample is different from the one on the pressure standard in the high-pressure x-ray diffraction measurements.

There are conflicting reports on the uncertainties of Holmes *et al.*'s EOS. Dewaele *et al.*[8] measured the EOS of six metals at ambient temperature to 94 GPa using a diamond-anvil cell (DAC). By cross-checking different pressure scales, they found Holmes *et al.*'s EOS overestimates pressure by ≈4 GPa near 100 GPa at room temperature. This conclusion is confirmed by other groups.[9,10] While more recent calculations based on density-functional theory (DFT) suggest that Holmes *et al.*'s EOS underestimates, rather than overestimates, pressure. Xiang *et al.*[11] computed the thermal equation of state of platinum using LMTO and a mean-field potential method. The pressure they obtained is 5%–6% higher than that of Holmes *et al.* at high pressures. Menéndez-Proupin and Singh[12] reached similar conclusion using pseudopotentials. Both calculations employ the local-density approximation (LDA) functional[13] and the excess pressure is attributed to LDA in Ref. 12. However it can also be caused by other factors. In Table 2 of Ref. 11, the equilibrium volume decreases as the temperature increases. The electronic thermal pressure is negative according to this calculation, which is contrary to expectations. Reference 12 uses an ultrasoft Rappe-Rabe-Kaxiras-Joannopoulos pseudopotential from the PWSCF website,[14] which contains only 5*d*, 6*s*, and 6*p* valence states. Its large cut-off radius (2.6 a.u.) may cause error in studying the highly compressed structure.

Besides the room-temperature isotherm, accurate thermal pressure (P_{th}) is needed to calibrate pressure in simultaneous high-pressure and high-temperature experiments. Experiments cannot easily determine P_{th} over a wide temperature and volume range.[15] Consequently P_{th} is often estimated by assuming it is linear in temperature and independent of volume.[1,4] Theory can in principle do better. In quasiharmonic approximation (QHA), DFT calculations give P_{th} at any particular temperature and volume. It is desirable to combine the experimental data with DFT calculations, taking the advantages of both, and construct a more accurate thermal EOS for pressure calibration.

In this paper we have three goals: first is to check the accuracy of the theoretical EOS of platinum predicted by different exchange-correlation functionals. In contrast with previous calculations, we find the room-temperature isotherm computed with LDA lies below and nearly parallel to the experimental compression data. The Fermi level of platinum lies in the *d* band and gives a very large density of state (DOS) $N(E_F)$. Its vibrational frequencies are more sensitive to the electronic temperature than those of many other metals. A Kohn anomaly has been observed in platinum at 90 K.[16] It becomes weaker and finally disappears when the temperature increases. Thus our second goal is to discuss the electronic temperature dependence of vibrations (ETDV) and its influence on the thermal properties. Our last goal is to provide an accurate thermal EOS for pressure calibration.

For this purpose we make corrections to the raw DFT results. We correct the room-temperature Gibbs free energy $G(P,300\ \mathrm{K})$ to ensure that it reproduces the experimental isotherm and then combine it with the DFT calculated temperature dependence to get $G(P,T)$. The thermal EOS and thermal properties deduced from the corrected Gibbs free energy are in good agreement with the known experimental data.

II. COMPUTATIONAL METHOD

The EOS of a material is determined by its Helmholtz free energy $F(V,T)$, which consists of three parts:

$$F(V,T) = U(V) + F_{\mathrm{vib}}(V,T) + F_{\mathrm{ele}}(V,T), \tag{1}$$

where $U(V)$ is the static energy of the lattice, $F_{\mathrm{vib}}(V,T)$ is the vibrational free energy, and $F_{\mathrm{ele}}(V,T)$ accounts for the thermal excitation of the electrons. $U(V)$ is calculated by using the linearized augmented plane-wave (LAPW) method[17] and three different exchange-correlation functionals: LDA,[13] Perdew-Burke-Ernzerhof (PBE),[18] and Wu-Cohen (WC).[19] The $4f$, $5s$, $5p$, $5d$, and $6s$ are described as valence states while others are treated as core states. The convergence parameter $RK_{\max}$ is 10.0 and the muffin-tin radius R is 2.08 a.u.. A $16\times16\times16$ Monkhorst-Pack[20] uniform k grid is used and the integration over the whole Brillouin zone is done with the tetrahedron method.[21] All the calculations using LAPW are performed with and without spin-orbit effect.

In contrast with the static lattice energy $U(V)$, which is sensitive to the relaxation of the core states and requires a full-potential treatment, thermal excitations contribute to much smaller energy variations and mostly depend on the valence states. We use pseudopotentials to compute the thermal effects. An ultrasoft Vanderbilt pseudopotential[22] is generated from the reference atomic configuration $5s^25p^65d^96s^16p^0$, including nonlinear core corrections.[23] There are two projectors in the s channel ($5s$ and $6s$), two in the p channel ($5p$ and an unbound p at 0.2 Ry above the vacuum level), and one in the d channel ($5d$). The local component is set in the f channel at the vacuum level. The cut-off radii for each channel s, p, d, and local are 1.8, 1.9, 1.9, and 1.8 a.u., respectively. We use the scalar relativistic approximation and the spin-orbit effect is not included. This pseudopotential reproduces the LAPW electronic band structure both at the most contracted volume and the 0 GPa experimental volume. We find that pseudopotentials with different exchange-correlation functionals yield very similar electronic band structures for platinum and we use LDA to compute all the thermal effects.

We consider 20 different volumes with lattice constants from 7.8 to 6.2 a.u.(17.58–8.83 Å^3 in volume). For each volume V_i, we use LAPW to compute its static energy $U(V_i)$ and the LDA pseudopotential to evaluate its thermal free energy $F_{\mathrm{vib}}(V_i,T)$ and $F_{\mathrm{ele}}(V_i,T)$. $F_{\mathrm{vib}}(V_i,T)$ is treated within QHA with phonon frequencies dependent on electronic temperature (denoted as eQHA) as

$$F_{\mathrm{vib}}^{\mathrm{eQHA}}(V_i,T) = \frac{1}{2}\sum_{\mathbf{q},j}\hbar\omega_{\mathbf{q},j}(V_i,T_{\mathrm{ele}}) + k_{\mathrm{B}}T\sum_{\mathbf{q},j}\ln\left\{1-\exp\left[\frac{-\hbar\omega_{\mathbf{q},j}(V_i,T_{\mathrm{ele}})}{k_BT}\right]\right\}, \tag{2}$$

where $\omega_{\mathbf{q},j}(V_i,T_{\mathrm{ele}})$ denotes the phonon frequency computed at volume V_i and electronic temperature T_{ele}. In thermal equilibrium the system temperature T, the ionic temperature T_{ion}, and the T_{ele} are equal. We distinguish these three temperatures to emphasize that the temperature dependence of phonon frequencies coming from different sources. Anharmonic phonon-phonon interactions cause phonon frequencies to depend on T_{ion} but they are omitted in QHA. Electronic thermal excitations disturb the charge distribution in the crystal and cause phonon frequencies dependent on T_{ele}. In the normal QHA used for insulators and some metals, this effect is also ignored and $\omega_{\mathbf{q},j}$ has no temperature dependence [except through $V(T)$]. Platinum has a larger $N(E_F)$ than many other metals and ETDV may have noticeable effects on its thermal properties. To quantitatively measure the influence of ETDV, we compare the vibrational free energies at volume V_i and temperature $T_j(T_j=500,1000,\ldots,5000\ \mathrm{K})$ computed without and with ETDV. Without ETDV (normal QHA), phonon frequencies are computed at $T_{\mathrm{ele}}=0$ K by using Methfessel-Paxton[24] (MP) smearing with a smearing parameter of 0.01 Ry. The corresponding vibrational free energy is denoted as $F_{\mathrm{vib}}^{\mathrm{QHA}}(V_i,T_j)$. With ETDV (eQHA), phonon frequencies have to be computed separately for each T_j. This is achieved by using the Mermin functional[25] and Fermi-Dirac (FD) smearing. The corresponding vibrational free energy is denoted as $F_{\mathrm{vib}}^{\mathrm{eQHA}}(V_i,T_j)$. The difference between these two, $\Delta F_{\mathrm{ETDV}}(V_i,T_j)=F_{\mathrm{vib}}^{\mathrm{eQHA}}(V_i,T_j)-F_{\mathrm{vib}}^{\mathrm{QHA}}(V_i,T_j)$, describes the correction caused by ETDV. To get ΔF_{ETDV} at arbitrary temperature between 0–5000 K, we fit a fourth order polynomial from $\Delta F_{\mathrm{ETDV}}(V_i,T_j)$,

$$\Delta F_{\mathrm{ETDV}}(V_i,T) = F_{\mathrm{vib}}^{\mathrm{eQHA}}(V_i,T) - F_{\mathrm{vib}}^{\mathrm{QHA}}(V_i,T) = a_1(V_i)\cdot T + a_2(V_i)\cdot T^2 + a_3(V_i)\cdot T^3 + a_4(V_i)\cdot T^4. \tag{3}$$

The final vibrational free energy is computed as $F_{\mathrm{vib}}(V_i,T) = F_{\mathrm{vib}}^{\mathrm{QHA}}(V_i,T)+\Delta F_{\mathrm{ETDV}}(V_i,T)$ (we omit the superscript "eQHA" and denote $F_{\mathrm{vib}}^{\mathrm{eQHA}}$ as F_{vib}).

Phonon frequencies in the above procedure are determined by density functional perturbation theory (DFPT) (Ref. 27), as implemented in the QUANTUM ESPRESSO (Ref. 28) package. The dynamical matrices are computed on an $8\times8\times8$ **q** mesh (29 **q** points in the irreducible wedge of the Brillouin zone). Force constant interpolation is used to calculate phonon frequencies at arbitrary **q** vectors. The summation in Eq. (2) is evaluated on a $32\times32\times32$ **q** mesh.

The electronic free energy $F_{\mathrm{ele}}(V_i,T)$ is determined by using the Mermin functional[25,26] and Fermi-Dirac smearing. Similar to getting $F_{\mathrm{vib}}(V_i,T)$, we first compute F_{ele} at every 50 K from 50 to 5000 K, then we fit them to a fourth order polynomial

$$F_{\mathrm{ele}}(V_i,T) = b_1(V_i)\cdot T + b_2(V_i)\cdot T^2 + b_3(V_i)\cdot T^3 + b_4(V_i)\cdot T^4. \quad (4)$$

Terms other than $b_2(V_i)T^2$ represent deviations from the lowest-order Sommerfeld expansion $F_{\mathrm{ele}} = -\frac{\pi^2}{6}N(E_F,V_i)(k_BT)^2$, where $N(E_F,V_i)$ is the electronic density of states at Fermi energy E_F and volume V_i. We find that, below 1000 K, keeping only the quadratic term does not introduce much error. The influence of the higher order terms becomes prominent at high temperatures. At 2000 K, the error reaches about 15%. The fitted quadratic coefficient $b_2(V_i)$ differs from the Sommerfeld value $-\frac{\pi^2}{6}N(E_F,V_i)k_B^2$ by 5% (V_i=8.83 Å^3) to 15% (V_i=15.63 Å^3). It seems the Sommerfeld expansion works better at high pressures where the electronic bands are more dispersive and $N(E_F)$ is smaller. We combine $F_{\mathrm{ele}}(V_i,T)$ with the static energy $U(V_i)$ from LAPW and the vibrational free energy $F_{\mathrm{vib}}(V_i,T)$ from the same pseudopotential to get the total free energy $F(V_i,T)$ at volume V_i. There are two popular parametrized forms to fit the total free energy $F(V,T)$: fourth order Birch-Murnahan[29] (BM) and Vinet.[30] We find BM and Vinet are comparable in accuracy to fit the static and low-temperature free energies but BM yields much lower residual energies than Vinet for the high-temperature results. Thus we use fourth order BM to get $F(V,T)$. Other thermodynamical properties are computed by finite difference.

All the pseudopotential calculations are carried out with the same plane-wave cutoff of 40 Ry, charge-density cutoff of 480 Ry, and a shifted $16\times16\times16$ Monkhorst-Pack mesh. To determine the convergence uncertainties of our results, we choose one volume (V_i=15.095 Å^3), and recompute its phonon frequencies at T_{ele}=0 K with a $24\times24\times24$ mesh and a higher plane-wave cutoff (60 Ry). The two sets of phonon frequencies differ by 0.5% at most. The corresponding $F_{\mathrm{vib}}^{\mathrm{QHA}}$ differ by 0.07 mRy/atom at 2000 K and 0.18 mRy at 5000 K. The influence of ETDV is much greater than the convergence uncertainties. For some modes phonon frequencies change by 10% or more from T_{ele}=500 K to T_{ele}=2000 K. The free-energy correction ΔF_{ETDV} is about 1 mRy/atom at 2000 K.

III. SUMMARY OF PREVIOUS WORKS

Besides the two calculations[11,12] mentioned in the introduction, which focus on the thermal EOS of platinum, there are some other papers related to this subject. Cohen *et al.*[31] computed the static EOS of platinum using LAPW and PBE, and treated it as an example to discuss the accuracy of different EOS formations. They found that Vinet fitted better than third order BM. The accuracy of fourth order BM and Vinet were comparable. Tsuchiya and Kawamura[32] computed the electronic thermal pressure (P_{ele}) of Au and Pt using LMTO and LDA. At 2200 K, P_{ele} is 1.01 GPa for Pt while only 0.06 GPa for Au. This is caused by the different $N(E_F)$ of the two metals. The small ETDV effect (1% change in phonon frequency from T_{ele}=0 K to 3000 K) observed on gold[33] is consistent with this picture. Wang *et al.*[34] used LAPW and an average potential method to determine the thermal contributions. Then they reduced the experimental shock Hugoniot and got the room-temperature isotherm of Pt. This isotherm is very similar to that of Holmes *et al.*, in spite of the fact that in the latter case, thermal pressure is estimated semiempirically. Reference 35 computed the static EOS of platinum using pseudopotentials with and without spin-orbit effects up to 150 GPa. In the following section, we compare our calculations with these previous ones whenever appropriate.

On the experimental side, The reduced isothermal *P-V-T* EOS from shock wave experiments are widely used as primary pressure scales. At present they are also the only experimental sources for *P-V-T* data at very high pressures. The shock Hugoniot of platinum was first obtained by using chemical explosives.[1] The reduced room-temperature isotherm was up to 270 GPa. Holmes *et al.*[4] went to higher compression ratio using a two-stage light-gas gun. The final shock Hugoniot is a combination of these two sets of data. In spite of the crucial role of the reduced shock EOS, its accuracy suffers from low precision in measurements and theoretical simplifications made in the reducing process.[10,36] With the development of DAC and third-generation synchrotron light source, cross-checking different pressure scales became feasible. More accurate thermal EOS were obtained by using this method.[8,15]

Recently, Dorogokupets and Oganov[37] constructed a semiempirical model to describe the thermal properties of Al, Au, Cu, Pt, Ta, and W. The model contains about 20 parameters, which are fitted to the available experimental data on the heat capacity, enthalpy, volume, thermal expansivity, bulk modulus, and shock Hugoniot. Based on this model, they reanalyzed the data in Ref. 8 up to 100 GPa. The resulting EOS, which are consistent with the measured thermal properties, are believed to be more accurate than the original in the corresponding pressure range.[38] A simplified version of the model[39] yields similar EOS at low pressures. However their high-pressure extrapolations differ by 2.5% near 240 GPa. It will be interesting to use DFT to explore the EOS at very high pressures, which are still out of reach for the current DAC experiments.

IV. RESULTS AND DISCUSSIONS

A. Static equation of state

Before studying the EOS at finite temperature, we examine the static EOS computed by using different exchange-correlation functionals and compare them with previous calculations. Excluding the thermal effects (which amount to $\approx$2 GPa at room temperature) helps to identify the origin of their differences. Figure 1 shows the static pressure vs volume relations using different exchange-correlation functionals. The corresponding EOS parameters are listed in Table I. The experimental data at room temperature are also included in the figure to give a rough estimate of the difference. Comparing to the experiments in the entire volume range, LDA underestimates pressure while PBE overestimates. WC improves on PBE but still overestimates. A detailed comparison between the calculated room-temperature isotherms (including the thermal effects) and the experimental data will be given in Sec. IV C. DFT has many different implementations

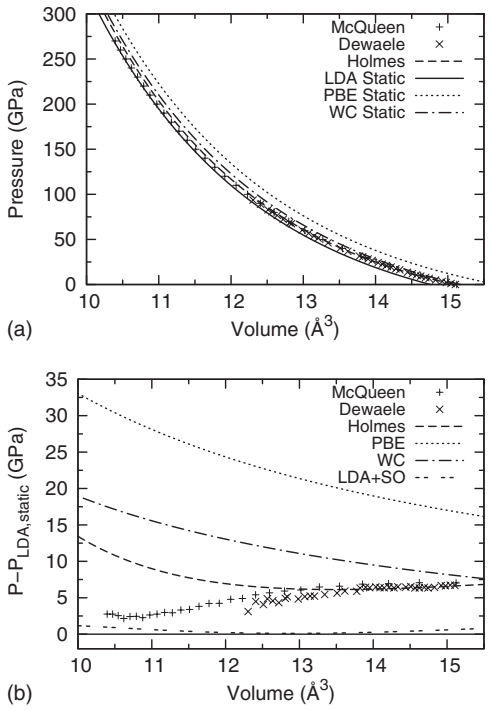

FIG. 1. Static EOS computed by the LAPW method using various exchange-correlation functionals. (a) Pressure vs volume curves. Spin-orbit effect is too small to be identified on this scale. (b) Pressure difference with respect to the static LDA EOS. In spite of the relative large change in EOS parameters, the actual pressure difference with and without spin-orbit effect is very small. Experimental data labeled as "McQueen" are from Ref. 1, "Dewaele" from Ref. 8, and "Holmes" from Ref. 4.

such as LAPW, LMTO, and various pseudopotentials. If the calculations are good, they should yield similar results. We compare our LDA calculations with previous ones in Fig. 2. Two of our own pseudopotential calculations are included for comparison. One is the Vanderbilt pseudopotential that we use to compute the thermal effects, denoted as pseudo-1. The other is a Rappe-Rabe-Kaxiras-Joannopoulos pseudopotential from the PWSCF website (Pt.pz-nd-rrkjus.UPF), denoted as pseudo-2. The static EOS predicted by pseudo-1 is similar to that of LAPW. Their EOS parameters differ by no more than 0.5%. The previous overestimations of pressure are probably caused by the large cut-off radius and insufficient number of valence electrons (Ref. 12), or another issue related to the negative electronic thermal pressure (Ref. 11).

Platinum is a heavy element and its electronic band structure is sensitive to spin-orbit effect.[41] We find inclusion of the spin-orbit effect increases the equilibrium volume no matter which exchange-correlation functional is used. This tendency has also been observed by Bercegeay and Bernard[35] in their pseudopotential calculations. However, the EOS parameters are not independent of each other. The variation of the equilibrium volume largely compensates that of the bulk modulus and the actual pressure difference is within 0.7% at high pressures.

Using pseudopotentials instead of the all electron LAPW may introduce error in computing phonon frequencies, especially at high pressures. Since lattice vibrations are closely related to the force (stress) on the atoms, we estimate the error in phonon frequencies by analyzing the error in static pressure. At high pressures (150–550 GPa), the pressure difference between LAPW (with LDA functional) and pseudo-1 is about 1.4%. The error in phonon frequencies caused by using pseudo-1 is likely to be of the same order. Since the influence of spin-orbit effect is half of the pseudopotential uncertainty, it is ignored completely in the following calculations.

B. Phonon dispersion and its electronic temperature dependence

Figure 3 shows the phonon dispersions at the experimental ambient condition lattice constant $a=7.4136$ a.u. [8] One is computed at $T_{ele}=0$ K while the other at $T_{ele}=2000$ K, close to platinum's melting point at ambient pressure 2041.3 K.[42] The Kohn anomaly (near $\mathbf{q}=[0,0.35,0.35]$) disappears when the electronic temperature is high and the vibrational DOS varies noticeably. The corresponding corrections to the vibrational free energy, $\Delta F_{\mathrm{ETDV}}(V_i,T)$, are shown in Fig. 4(a). ΔF_{ETDV} is always positive. As volume decreases, it diminishes and finally becomes negligible. ETDV originates in the thermal excitations of the electrons near the Fermi surface and the number of thermal excited electrons is proportional to $N(E_F)$ in the lowest-order Sommerfeld expansion. For smaller volumes, the electronic bands are more dispersive and $N(E_F)$ decreases, as shown in Fig. 4(b). ETDV diminishes accordingly.

Figures 5 and 6 show the volume thermal-expansion coefficient α, heat capacity at constant pressure C_P, entropy S, and the temperature-dependent part of the Gibbs free energy $\Delta G(P,T)=G(P,T)$-$G(P,T=300\ \mathrm{K})$. Including ETDV removes about half of the discrepancies between experiments and calculations based on normal QHA. The remaining small differences between theory and experiment are attributed to anharmonic phonon-phonon interactions[43] and electron-phonon interactions.[44] These two effects are of the same order of magnitude[44] as F_{ele} for metals. But explicit perturbative calculations to determine their magnitudes are computationally demanding and beyond the scope of the current paper. We notice DFT calculations based on QHA describe well the thermal properties of other metals, such as gold,[33] silver,[45] and copper,[46] up to melting point. This is in contrast with ionic crystals such as MgO where there are large deviations from QHA at high temperatures. It is possible that the effects of anharmonic phonon-phonon and electron-phonon interactions tend to cancel each other in these metals. Further work is needed to clarify this issue.

C. Room-temperature isotherms

By fitting the total Helmholtz free energy at 300 K, we get the theoretical 300 K isotherms, as shown in Fig. 7. Their parameters are listed in Table II. In the low-pressure range, the LDA isotherm and the experimental data are almost parallel. As pressure increases, they start to merge. It seems LDA works better at high pressures. Regarding to EOS parameters, LDA gives equilibrium volumes closest to the experiments while WC yields closest bulk modulus (K_0) and

TABLE I. Static EOS parameters obtained from LAPW calculations and compared with those in literature. Parameters from the pseudopotential calculations (pseudo-1 and pseudo-2) are also listed. For convenience, both Vinet and fourth order BM parameters are shown. V_0 denotes the equilibrium volume, and K_0, K_0', and K_0'' are the isothermal bulk modulus, the first and second derivatives of the bulk modulus at V_0, respectively. Note their different fitting ranges: 0–550 GPa (this study), 0–1000 GPa (Ref. 11), 0–660 GPa (Ref. 12), 0–150 GPa (Ref. 35), and 0–350 GPa (Ref. 31). Reference 35 uses third order BM EOS so the corresponding K_0'' are not listed.

	Vinet			B-M			
	V_0 (Å^3)	K_0 (GPa)	K_0'	V_0(Å^3)	K_0 (GPa)	K_0'	K_0'' (GPa^{-1})
LDA	14.752	308.02	5.446	14.761	309.29	5.295	–0.02666
LDA+SO	14.784	301.17	5.533	14.785	301.13	5.510	–0.03214
LDA (pseudo-1)	14.719	308.69	5.423	14.726	309.61	5.295	–0.02681
LDA (pseudo-2)	15.055	297.48	5.515	15.060	299.28	5.375	–0.02873
LDA[a]	14.90	300.9	5.814				
LDA[b]	15.073	293	5.56				
LDA[c] (HGH)				14.82	305.99	5.32	
LDA+SO[c,d] (TM)				15.2	291.18	5.35	
PBE	15.679	242.50	5.639	15.678	245.88	5.464	–0.03620
PBE+SO	15.751	231.97	5.762	15.754	229.96	5.850	–0.04932
PBE[a]	15.77	243.3	5.866				
PBE[c] (HGH)				15.59	250.85	5.65	
PBE[e]	15.69	248.9	5.43				
WC	15.171	280.63	5.500	15.177	283.49	5.306	–0.02889
WC+SO	15.223	269.97	5.630	15.223	269.00	5.670	–0.03893

[a]Reference 11.
[b]Reference 12.
[c]Reference 35.
[d]Reference 40.
[e]Reference 31.

the derivative of the bulk modulus (K_0'). Some people[8,35] prefer to compare pressures from two EOS (labeled as EOS-I and EOS-II) at the same compression, i.e., the same value of V/V_0. V_0 is the corresponding equilibrium volume, $V_{0,\mathrm{I}}$ for EOS-I, and $V_{0,\mathrm{II}}$ for EOS-II. Such comparisons can give favorable agreement when K_0 and K_0' of EOS-I are close to those of EOS-II even when $V_{0,\mathrm{I}}$ and $V_{0,\mathrm{II}}$ are quite different.[8] As mentioned before, the EOS parameters are not independent of each other. It can be fortuitous that K_0 and K_0' agree well. Judged from pressure vs volume relation, LDA is the optimal functional for platinum. It is worth noting that the LDA Hartwigsen, Goedecker and Hutter (HGH) pressure vs volume relation reported in Ref. 35 is similar to those obtained in this study. However, Ref. 35 presents data in volume vs compression and concludes that LDA overestimates pressure by 8 GPa near 100 GPa. In fact, although $K_{0,\mathrm{LDA}}$ (291 GPa from this study) is much larger than $K_{0,\mathrm{expe}}$ (273.6 GPa from Ref. 8), the bulk modulus computed at the experimental equilibrium volume $V_{0,\mathrm{expe}}$(15.095 Å^3) is 270 GPa, quite close to $K_{0,\mathrm{expe}}$. Thus when plotted in pressure vs volume, the isotherm computed by LDA is nearly parallel with the experimental data in the low-pressure range.

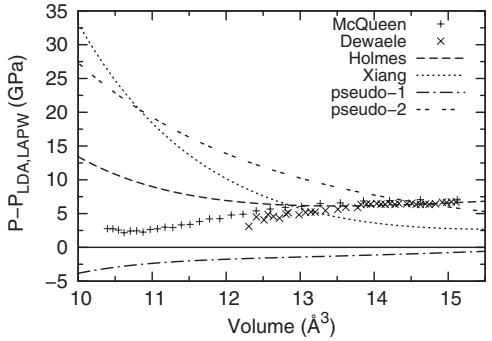

FIG. 2. Different LDA static EOS compared with the one computed by using LAPW. "Xiang" denotes the EOS from Ref. 11.

D. Thermal equation of state of platinum for pressure calibration

In the previous sections the thermal properties of platinum is discussed from a pure theoretical point of view. We have computed the static lattice energy $U(V)$ using LAPW and found that spin-orbit interactions are not important in determining the EOS of platinum. We have used QHA to calculate the vibrational free energy $F_{\mathrm{vib}}(V,T)$ and found that including ETDV improves the agreement on the thermal properties. We have calculated the electronic free energy $F_{\mathrm{ele}}(V,T)$ using Mermin functional. The resulting thermal properties, e.g., the temperature-dependent part of the Gibbs energy $\Delta G(P,T)$, are close to the experimental data at 0 GPa. The

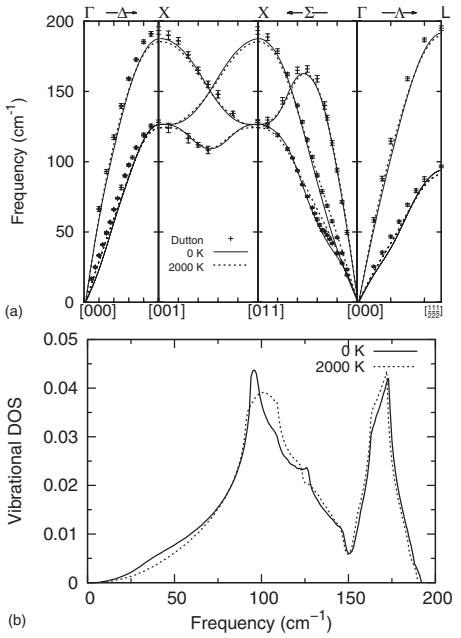

FIG. 3. (a) Phonon dispersion and (b) vibrational DOS at a =7.4136 a.u. Solid line corresponds to T_{ele}=0 K and dashed line corresponds to T_{ele}=2000 K. They are calculated by using the LDA pseudopotential. Experimental data labeled as "Dutton" are from Ref. 16.

room-temperature isotherm computed by LDA merges to the reduced shock data at high pressures, indicating LDA works better at high pressures.

Based on these DFT results and all the available experimental data, we try to construct a consistent P-V-T EOS of platinum up to 550 GPa and 5000 K. To reach this goal, first

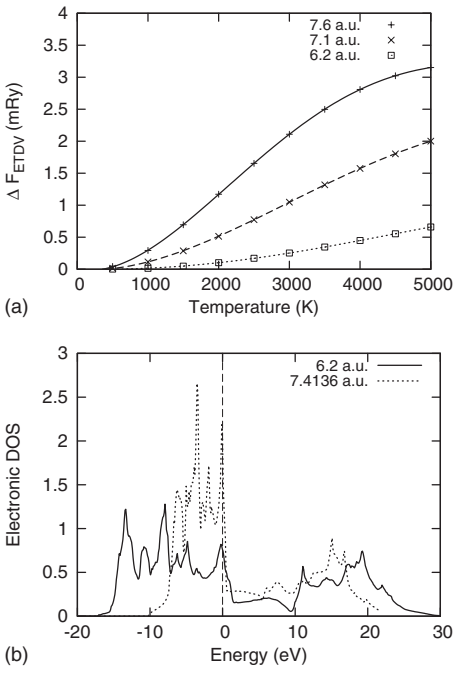

FIG. 4. (a) Corrections to the vibrational free energy at various lattice constants. (b) Volume dependence of the electronic density of states.

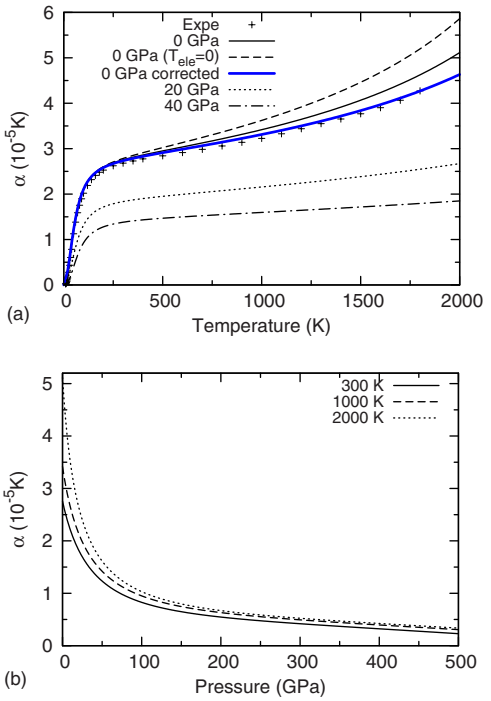

FIG. 5. (Color online) Thermal expansivity as a function of (a) temperature and (b) pressure. Curves with label (T_{ele}=0) represent properties computed without ETDV, i.e., computed from F_{vib}^{QHA}. Curves without this specification are the default ones computed with ETDV. "0 GPa corrected" denotes the results obtained by adding a phenomenological correction to account for anharmonic phonon-phonon and electron-phonon interactions. These corrected thermal data are used to construct the final thermal EOS in Tables III and IV. The experimental data are from Ref. 47.

we need to include the physical effects that are missing in our original model. A phenomenological term[39] $\Delta F_{corr}(V,T)=-\frac{3}{2}k_B a(V/V_0)^m T^2$ is added to the total Helmholtz energy to account for the anharmonic phonon-phonon and electron-phonon interactions where V_0 is the volume of a primitive cell at ambient condition (V_0=15.095 Å^3). The quadratic temperature dependence comes from the lowest-order perturbation at high temperatures. a and m are two parameters to be fitted. We found that setting a as equal to 10^{-5}K^{-1} and m as equal to 7 yields good agreement between theory and experiments on α, C_P, and $\Delta G(P,T)$ at 0 GPa, as illustrated in Figs. 5(a) and 6(a). The contribution to thermal pressure can be estimated by differentiating $\Delta F_{corr}(V,T)$ with respect to volume. At 2000 K, ΔP_{th} is 0.38 GPa when V is equal to V_0 and 0.2 GPa when V is equal to $0.9V_0$.

Having obtained accurate $\Delta G(P,T)$, the next step is to get reliable $G(P,300\ \text{K})$. We choose the room-temperature EOS developed by Dorogokupets and Oganov[37] as our reference below 100 GPa. It has been cross-checked with other pressure scales and is likely to be more accurate than the reduced shock data of Ref. 1 in this pressure range. On the other hand, extrapolating an EOS fitted at low pressures to higher range can be dangerous. We assume LDA works better at high pressures, and the difference between the exact (obtained in an ideal, very accurate experiment) and LDA isotherms approaches to zero as pressure increases.

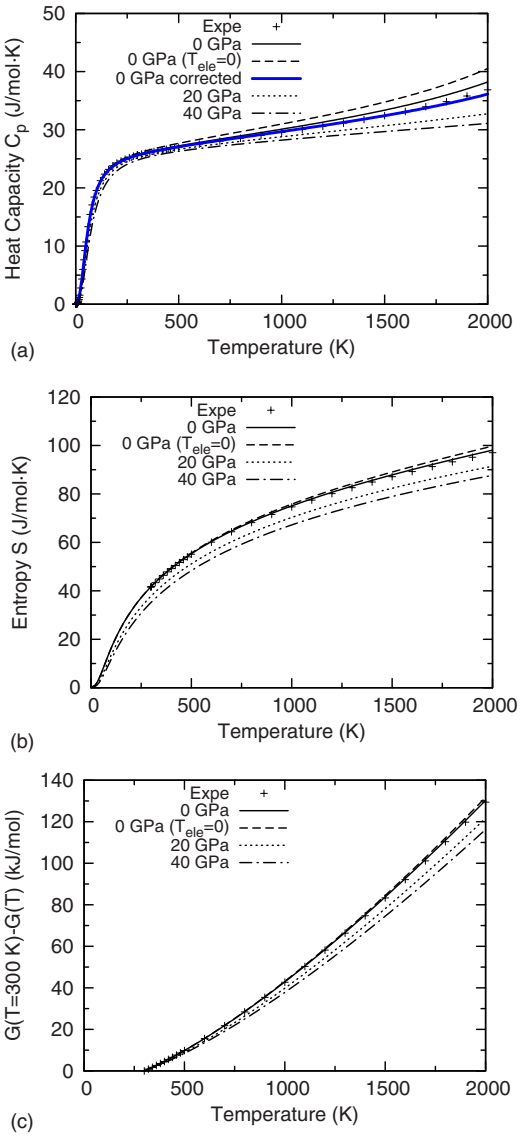

FIG. 6. (Color online) Thermal properties of platinum. (a) Heat capacity at constant pressure, (b) entropy, and (c) temperature dependence of the Gibbs free energy at constant pressure. The meanings of the labels are the same as above. On this scale it is difficult to discern the improvements on entropy and Gibbs free energy, caused by including the phenomenological correction on anharmonic phonon-phonon and electron-phonon interactions. Thus those data are not shown. The experimental data are from Ref. 48.

We compare Dorogokupets's EOS (Ref. 37) (V_0 =15.095 Å^3, K_0=276.07 GPa, and K_0'=5.30 in Vinet form) with our room-temperature isotherm computed by LDA (V_0 =14.884 Å^3, K_0=291.25 GPa, and K_0'=5.547 in Vinet form). The volume difference between these two at each pressure $\Delta V(P)=V_{\text{expe,300 K}}(P)-V_{\text{LDA,300 K}}(P)$ is shown in Fig. 8. Since $\Delta V(P)$ decreases rapidly as pressure increases, we use exponentially decaying functions to fit and extrapolate. We correct the calculated room-temperature Gibbs energy $G_{\text{LDA}}(P,300\ \text{K})$ by setting $G_{\text{corr}}(P,300\ \text{K})$ $=G_{\text{LDA}}(P,300\ \text{K})+\int_0^P \Delta V(P)dP$. The isotherm derived from $G_{\text{corr}}(P,300\ \text{K})$ coincides with Dorogokupets' EOS below 100 GPa, which is the upper limit of their fitting. Above 250 GPa, $\Delta V(P)$ is almost zero and the isotherm derived from $G_{\text{corr}}(P,300\ \text{K})$ is the same as the uncorrected one. The uncertainty due to volume extrapolation in the intermediate region (100–250 GPa) is estimated from bulk modulus to be less than 2 GPa. It is worth noting that the established EOS of platinum are quite similar to each other below 100 GPa, as shown in Fig. 7(b). Choosing a different reference such as the one in Ref. 8 will only change the results near 100 GPa by 1 GPa.

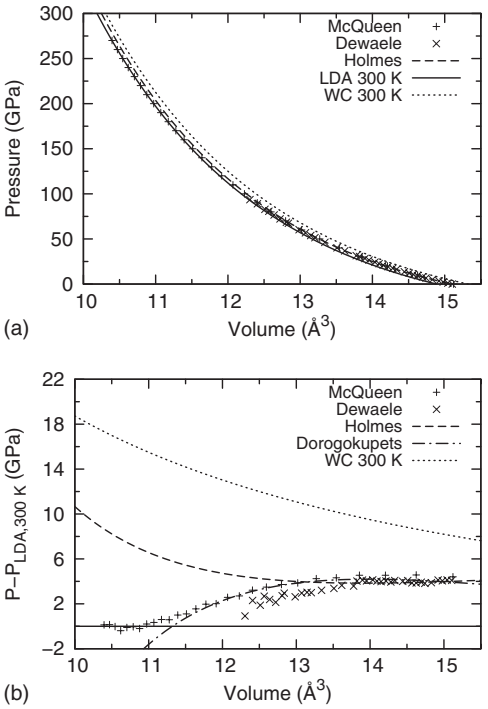

FIG. 7. 300 K isotherms. (a) Pressure vs volume. (b) Pressure difference. "Dorogokupets" denotes EOS from Ref. 37, which is very close to the reduced shock EOS (McQueen) near 100 GPa. PBE is not plotted as its EOS is way off.

We combine $G_{\text{corr}}(P,300\ \text{K})$ with the temperature-dependent part of the Gibbs energy $\Delta G(P,T)$ and get the corrected Gibbs energy $G_{\text{corr}}(P,T)$ at temperature T. From $G_{\text{corr}}(P,T)$, we derive all the other thermodynamical properties. Thermal properties such as α, C_P, and S, which depend on the temperature derivatives of the Gibbs energy, are not affected by changing $G(P,300\ \text{K})$. In contrast, the isothermal bulk modulus K_T and adiabatic bulk modulus K_S will be influenced, as shown in Fig. 9.

After corrections, both thermal expansivity and bulk modulus agree with the experiments well. We expect the product αK_T to be accurate. Integrating αK_T, we get the thermal pressure, $P_{\text{th}}(V,T)=P(V,T)-P(V,T_0)=\int_{T_0}^{T}\alpha K_T dT$. The calculated αK_T and P_{th}, both before and after corrections, are shown in Fig. 10. $P_{\text{th}}(V,T)$ is often assumed to be independent of volume and linear in temperature, i.e., αK_T is a constant. Reference 1 assumes the thermal energy $E(T)=3k_BT$, the thermal Grüneisen parameter $\gamma=\gamma_0 V/V_0$, where $\gamma_0=2.4$, and $V_0=15.123$ Å^3. The thermal pressure is obtained from Mie-Grüneisen relation,

TABLE II. EOS parameters of the theoretical 300 K isotherms, compared with the experiments. $V_{0,\mathrm{expe}}$ is 15.095 Å^3. Pressure range: 0–550 GPa (this study), 0–660 GPa (Refs. 4 and 12), 0–94 GPa (Refs. 8 and 37), and 0–270 GPa (Ref. 1).

	Vinet			B-M			
	V_0 (Å^3)	K_0 (GPa)	K_0'	V_0 (Å^3)	K_0 (GPa)	K_0'	K_0'' (GPa^{-1})
LDA	14.884	291.25	5.547	14.886	291.65	5.496	−0.03232
LDA ($V_{0,\mathrm{expe}}$)		269.96	5.640		269.91	5.626	−0.03730
LDA[a]	15.188	281	5.61				
PBE	15.864	225.55	5.751	15.866	225.34	5.741	−0.04709
WC	15.322	263.93	5.601	15.325	264.72	5.530	−0.03580
Holmes[b]	15.10	266	5.81				
Dewaele[c]	15.095	273.6	5.23				
Dorogokupets[d]	15.095	276.07	5.30				
McQueen[e]				15.123	277.715	4.821	−0.01379

[a]Reference 12.
[b]Reference 4.
[c]Reference 8. When K_0 is set to 277 GPa, the value measured by ultrasonic experiments, K_0' is equal to 5.08 GPa.
[d]Reference 37, improved analysis using data from Ref. 8.
[e]Reference 1. Fitted from the tabulated shock reduced isotherm at 293 K.

$$P_{\mathrm{th}}(V,T) = \frac{E(T)\gamma(V)}{V} = \frac{3k_B\gamma_0}{V_0}\cdot T = 6.57\times 10^{-3}\cdot T(\mathrm{GPa}). \tag{5}$$

In Ref. 4, αK_T is estimated to be 6.94×10^{-3} GPa/K. Both values lie within the variation of the calculated αK_T, as shown in Fig. 10(a). We find that $\alpha K_T(P_{\mathrm{th}})$ has noticeable volume dependence. At fixed temperature, it first decreases, reaches a minimum at about $V/V_0=0.8$, and then increases. Such behavior originates in the pressure dependence of the thermal expansivity [Fig. 5(b)] and bulk moduli [Fig. 9(b)]. This feature has also been observed in Ref. 37, as shown in Fig. 10(b). However it is missing in the previous *ab initio* calculation.[11]

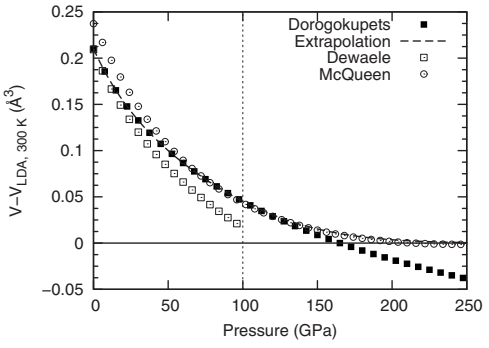

FIG. 8. Volume correction to the theoretical isotherm at 300 K. We use $\Delta V(P)=0.1215\cdot\exp(-P/34.0846)+0.0885\cdot\exp[-(P/109.989)^2]$ to fit the volume difference in the range $P<100$ GPa. The exponential functional form guarantees that it approaches zero at high pressures. It happens that this extrapolation agrees well with McQueen's reduced shock data.

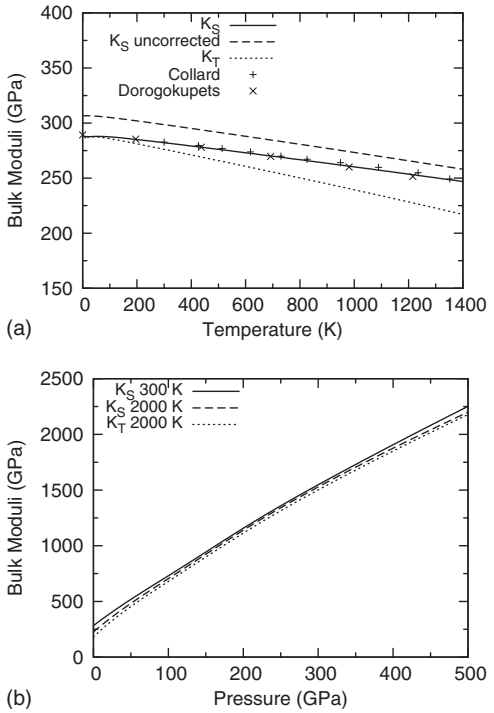

FIG. 9. (a) Bulk moduli at 0 GPa. "Uncorrected" denotes the raw DFT results without any correction. As noted in Ref. 37, the experimental data in Ref. 49 is inconsistent. The data points we show here are digitized from the graphs in Refs. 49 (denoted as "Collard") and 37 (denoted as Dorogokupets), respectively. K_S deduced from the corrected Gibbs free energy agrees well with the one computed from empirical models in Ref. 37. (b) Bulk moduli as a function of pressure.

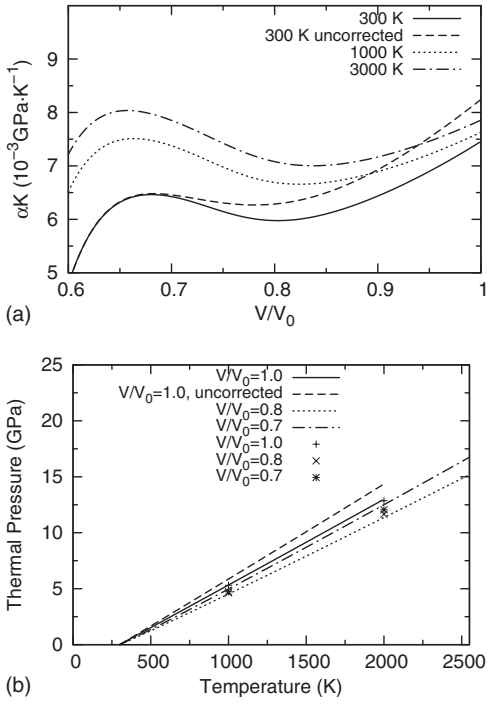

FIG. 10. (a) Temperature derivative of P_{th}, $\alpha K_T = \frac{\partial P_{\mathrm{th}}}{\partial T}$, before and after corrections. (b) Thermal pressure P_{th} at different V/V_0 where V_0 is the experimental volume at ambient condition (15.095 Å^3). Points are the thermal pressures from Ref. 37.

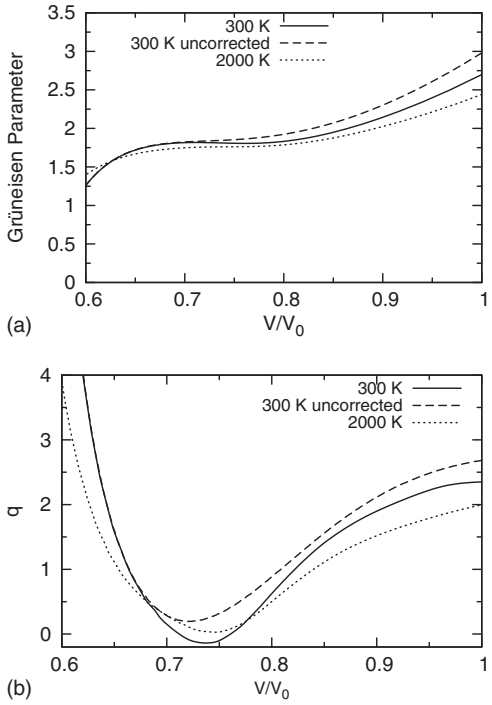

FIG. 11. Thermal Grüneisen parameter (a) volume dependence at fixed temperature. (b) The corresponding q.

Thermal Grüneisen parameter $\gamma = \frac{\alpha K_T V}{C_V}$ is an important quantity. Empirically it is often assumed to be independent of temperature. Its volume dependence is described by a parameter $q = \frac{\partial \ln \gamma}{\partial \ln V}$ and γ can be represented in q as $\gamma = \gamma_0 (\frac{V}{V_0})^q$. From Mie-Grüneisen relation, it is obvious that q is related to the volume dependence of αK_T. If q is equal to 1, αK_T is independent of volume. If q is greater than 1, αK_T gets smaller as volume decreases. In Ref. 1 q is assumed to be equal to 1. Fei *et al.*[9] determined γ by fitting the measured $P-V-T$ data to the Mie-Grüneisen relation up to 27 GPa. They gave $\gamma_0 = 2.72$ and $q = 0.5$. Zha *et al.*[10] extended measurements to 80 GPa and 1900 K. Their fit gave $\gamma_0 = 2.75$ and $q = 0.25$. Our calculation indicates that the temperature dependence of γ is small. The volume dependence of γ is shown in Fig. 11. The uncorrected DFT calculation tends to overestimate γ. At ambient condition γ_0 is equal to 2.87. After corrections, $\gamma_0 = 2.70$. The corresponding q is equal to 2.35, much larger than the value obtained in Refs. 9 and 10. We notice previous DFT calculation on gold[33] also gives much larger q than the value in Ref. 9. This is probably due to the small pressure range explored in Ref. 9 and limited number of data points measured in Ref. 10.

Adding the thermal pressure to the room-temperature isotherm, we get the thermal EOS of platinum, as shown in Table III. We compare our results with two DAC measurements in Fig. 12. Within the error of the experiments, the

TABLE III. Pressure (in GPa) as a function of compression ($1-V/V_0$, V_0 is the experimental volume at ambient condition; 15.095 Å^3) and temperature (in K), deduced from the corrected Gibbs free energy. Pressures above melting point is not shown. The melting point is determined using $T_m(P) = 2057 + 27.2 \times P - 0.1497 \times P^2$ K up to 70 GPa from Ref. 42

$1-V/V_0$	300	500	1000	1500	2000	2500	3000	3500	4000	4500	5000
0.00	0.00	1.51	5.31	9.14	12.97						
0.05	16.22	17.62	21.20	24.83	28.48	32.16					
0.10	38.32	39.64	43.05	46.52	50.03	53.57	57.14				
0.15	68.41	69.67	72.97	76.34	79.77	83.24	86.73	90.25			
0.20	109.46	110.71	113.99	117.37	120.82	124.31	127.83	131.39	134.98		
0.25	166.45	167.74	171.15	174.69	178.29	181.94	185.63	189.36	193.13	196.94	200.81
0.30	247.37	248.72	252.34	256.07	259.88	263.73	267.64	271.58	275.57	279.58	283.63
0.35	362.30	363.65	367.31	371.10	374.98	378.91	382.90	386.94	391.01	395.12	399.25
0.40	525.86	526.93	530.04	533.39	536.86	540.40	543.99	547.62	551.28	554.99	558.76

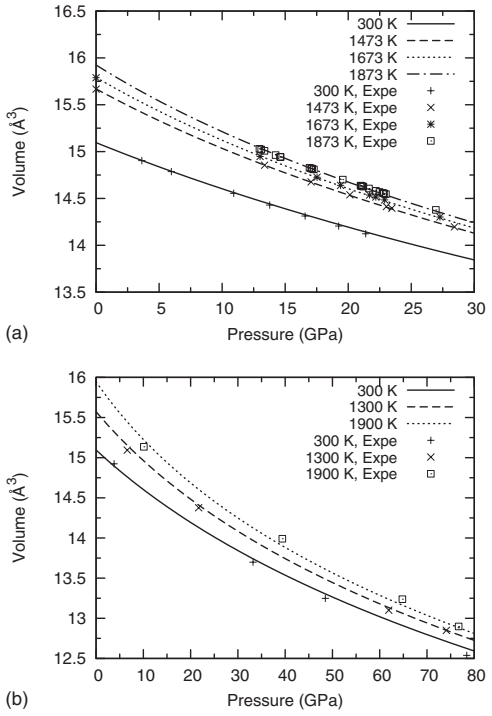

FIG. 12. High temperature isotherms after corrections. Lines correspond to the calculated isotherms. The experimental data in (a) are taken from Ref. 15 except those at $P=0$ GPa, which are obtained by integrating the thermal expansivity listed in Ref. 47. Data in (b) are from Ref. 10.

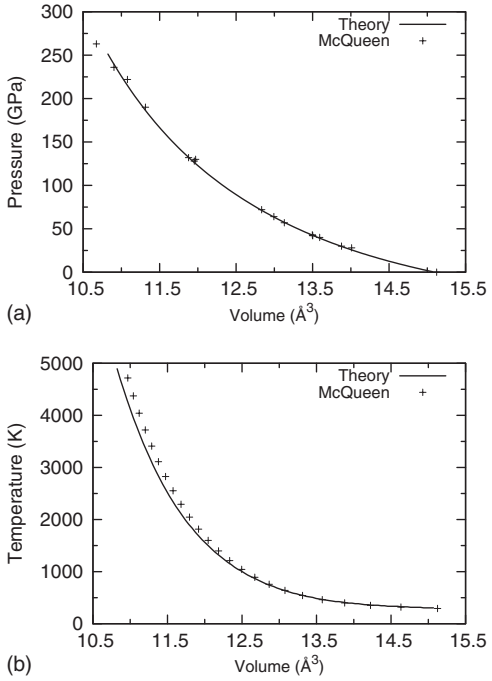

FIG. 13. (a) Theoretical shock Hugoniot compared with the experimental data from McQueen *et al.* (Ref. 1). (b) Temperature along the Hugoniot.

agreement is reasonably good. For convenience of interpolation, parametric forms of the thermal EOS are listed in Table IV.

The *P-V-T* thermal EOS we obtained are very similar to the one in Ref. 37 below 100 GPa. This is to be expected as we used the 300 K isotherm in Ref. 37 as the reference to correct the room-temperature Gibbs energy and the thermal properties calculated from both approaches agree well with the experiments. In this *P-T* range, the uncertainty of our EOS is comparable to the one in Ref. 37. Above 100 GPa, the uncertainty is about 1.4%, which is the difference between the LAPW (LDA) and pseudo-1 static EOS. Other sources of error, e.g., convergence uncertainty (0.5%) and ignoring spin-orbit effect (0.7%) are smaller effects. To check the accuracy of our thermal EOS at high pressures, we start from the corrected Gibbs energy and compute the theoretical Hugoniot by solving the Rankine-Hugoniot equation:

$$E_H(V,T) - E_i(V_0,T_i) = [P_H(V,T) + P_0(V_0,T_i)]\frac{V_0 - V}{2}, \quad (6)$$

where $E_H(V,T)$ and $P_H(V,T)$ are the internal energy, pressure at volume V, and temperature T. $E_i(V_0,T_i)$ and $P_0(V_0,T_i)$ are the internal energy, pressure at the initial volume V_0, and temperature T_i. The results are shown in Fig. 13. The predicted Hugoniot pressure is in good agreement with measurements. The temperature predicted by DFT is lower than the empirically deduced value in Ref. 1. The reduction in Ref. 1 neglects the electronic thermal pressure and this may cause the overestimation of Hugoniot temperature.[4]

We end this section by comparing our room-temperature isotherm with that of Holmes *et al.* Below 70 GPa, they are almost identical. At high pressures (200–550 GPa), the pressure from our EOS is about 3% lower than the one from Holmes *et al.* Holmes *et al.* used LMTO with the atomic-sphere approximation to get the static EOS. In principle, the full potential LAPW method used in this study is more accurate. It seems the EOS of Holmes *et al.* overestimates pressure systematically at high compression ratio. However, the magnitude is much smaller than the pressure offset needed to compensate the discrepancy between Mao *et al.*'s experiment and seismological extrapolation. The real cause of the discrepancy might be a combination of several factors.

V. CONCLUSIONS

In this paper, we report our calculations on the static and thermal EOSs of platinum using DFT with different exchange-correlation functionals. Contrary to previous reports, we found that the room-temperature isotherm computed with LDA lies below and nearly parallel to the experimental compression data. We studied the lattice dynamics of platinum within QHA and found that the electronic temperature dependence of vibrations plays a noticeable role in determining the thermal properties of platinum. Combining the experimental data with DFT calculations, we propose a consistent thermal EOS of platinum up to 550 GPa and 5000 K, which can be used as a reference for pressure calibration.

TABLE IV. Parametric form of the thermal EOS, $P(V)=P_0+\frac{3}{2}K_0[(V/V_0)^{-\frac{7}{3}}-(V/V_0)^{-\frac{5}{3}}]\cdot\{1+\frac{3}{4}(K_0'-4)[(V/V_0)^{-\frac{2}{3}}-1]+\frac{3}{8}[K_0K_0''+(K_0'-3)(K_0'-4)+\frac{35}{9}][(V/V_0)^{-\frac{2}{3}}-1]^2\}$. At high temperatures, the equilibrium volume may exceed the largest volume we calculated. For better accuracy we fit the P-V-T data in three different pressure-temperature intervals: (1) 0–100 GPa and 0–2000 K, (2) 50–250 GPa and 0–3000 K, and (3) 150–550 GPa and 0–5000 K. P_0 denotes the starting pressure of the corresponding interval. V_0 , K_0, K_0', and K_0'' are temperature-dependent parameters, and are fitted to a fourth order polynomial $a_0+a_1t+a_2t^2+a_3t^3+a_4t^4$, where $t=T/1000$. They have a formal correspondence to the usual fourth order BM EOS parameters, which are defined at $P_0=0$ GPa.

(1)	a_0	a_0	a_1	a_2	a_3
V_0 (Å^3)	14.9924	0.295837	0.194441	−0.0917141	0.024365
K_0 (GPa)	290.539	−45.4082	−9.38792	5.09573	−1.40266
K_0'	5.11956	0.52903	0.0733263	−0.0195011	0.0229666
K_0'' (GPa^{-1})	−0.0275729	−0.0120014	−0.0114928	0.00672243	−0.00359317
(2)	a_0	a_1	a_2	a_3	a_4
V_0 (Å^3)	13.2246	0.128227	0.049052	−0.0160359	0.00241857
K_0 (GPa)	523.48	−30.3849	−3.86087	1.31313	−0.222027
K_0'	4.24183	0.217262	−0.0235333	0.00944835	−0.000371746
K_0'' (GPa^{-1})	−0.00125873	−0.00268918	2.13874e−05	−3.57657e−05	−1.75847e−05
(3)	a_0	a_1	a_2	a_3	a_4
V_0 (Å^3)	11.4929	0.0672156	0.0119585	−0.00243269	0.000219022
K_0 (GPa)	951.004	−21.0874	−2.84254	0.654708	−0.0639296
K_0'	4.31383	0.05775	−0.00505386	0.00245414	−0.000167453
K_0'' (GPa^{-1})	−0.00588145	−0.00130468	0.000221904	−6.51359e−05	4.99978e−06

ACKNOWLEDGMENTS

We thank P. B. Allen, P. I. Dorogokupets, A. Floris, and B. B. Karki for discussions and help. We also thank A. Dewaele for suggestions and taking Ref. 39 to our attention, and Y. W. Fei for sending us Ref. 10. We are indebted to the anonymous referees for careful reviews. The pseudopotential calculations were performed at the Minnesota Supercomputing Institute (MSI) with the QUANTUM ESPRESSO package (http://www.pwscf.org). The LAPW calculations were performed at Brookhaven National Laboratory (BNL) with the WIEN2K package (http://www.wien2k.at). T.S. was supported by NSF/ITR Grant No. ATM0426757. R.M.W., K.U., and Z.W. were supported by NSF/EAR Grants No. 0230319 and No. 0635990, and NSF/ITR Grant No. 0428774 (VLab).

*tsun@grad.physics.sunysb.edu

[1] R. G. McQueen, S. P. Marsh, J. W. Taylor, J. M. Fritz, and W. J. Carter, in *High Velocity Impact Phenomena*, edited by R. Kinslow (Academic, New York, 1970), Chap. 7.

[2] J. A. Morgan, High Temp. - High Press. **6**, 195 (1974).

[3] J. C. Jamieson, J. N. Fritz, and M. H. Manghnani, in *High-Pressure Research in Geophysics*, edited by S. Akimoto and M. H. Manghnani (Center for Academic, Tokyo, 1982).

[4] N. C. Holmes, J. A. Moriarty, G. R. Gathers, and W. J. Nellis, J. Appl. Phys. **66**, 2962 (1989).

[5] H. K. Mao, Y. Wu, L. C. Chen, and J. F. Shu, J. Geophys. Res. **95**, 21737 (1990).

[6] F. D. Stacey and P. M. Davis, Phys. Earth Planet. Inter. **142**, 137 (2004).

[7] A. K. Singh, Phys. Earth Planet. Inter. **164**, 75 (2007).

[8] A. Dewaele, P. Loubeyre, and M. Mezouar, Phys. Rev. B **70**, 094112 (2004).

[9] Y. W. Fei, A. Ricolleau, M. Frank, K. Mibe, G. Shen, and V. Prakapenka, Proc. Natl. Acad. Sci. U.S.A. **104**, 9182 (2007).

[10] C. S. Zha, K. Mibe, W. A. Bassett, O. Tschauner, H. K. Mao, and R. J. Hemley, J. Appl. Phys. **103**, 054908 (2008).

[11] S. K. Xiang, L. C. Cai, Y. Bi, F. Q. Jing, and S. J. Wang, Phys. Rev. B **72**, 184102 (2005).

[12] E. Menéndez-Proupin and A. K. Singh, Phys. Rev. B **76**, 054117 (2007).

[13] J. P. Perdew and A. Zunger, Phys. Rev. B **23**, 5048 (1981).

[14] There are two LDA ultrasoft Rappe-Rabe-Kaxiras-Joannopoulos pseudopotentials on the PWSCF (www.pwscf.org) website. "Pt.pz-rrkjus.UPF" is the one without nonlinear core correction. "Pt.pz-nd-rrkjus.UPF" includes this correction. Both have a cutoff radius of 2.6 a.u. and both yield static EOS stiffer than that of N. C. Holmes *et al.* (Ref. 4). The results reported in Ref. 12 are very close to our calculations using 'Pt.pz-nd-rrkjus.UPF'.

[15] Y. W. Fei, J. Li, K. Hirose, W. Minarik, J. V. Orman, C. Sanloup, W. V. Westrenen, T. Komabayashi, and K. Funakoshi, Phys. Earth Planet. Inter. **143-144**, 515 (2004).

[16] D. H. Dutton, B. N. Brockhouse, and A. P. Miller, Can. J. Phys. **50**, 2915 (1972).

[17] P. Blaha, K. Schwarz, G. K. H. Madsen, D. Kvasnicka, and J. Luitz, in *WIEN2k: An Augmented Plane Wave and Local Orbitals Program for Calculating Crystal Properties*, edited by K. Schwarz (Vienna University of Technology, Vienna, Austria, 2001).
[18] J. P. Perdew, K. Burke, and M. Ernzerhof, Phys. Rev. Lett. **77**, 3865 (1996).
[19] Z. Wu and R. E. Cohen, Phys. Rev. B **73**, 235116 (2006).
[20] H. J. Monkhorst and J. D. Pack, Phys. Rev. B **13**, 5188 (1976).
[21] P. E. Blöchl, O. Jepsen, and O. K. Andersen, Phys. Rev. B **49**, 16223 (1994).
[22] D. Vanderbilt, Phys. Rev. B **41**, 7892 (1990).
[23] S. G. Louie, S. Froyen, and M. L. Cohen, Phys. Rev. B **26**, 1738 (1982).
[24] M. Methfessel and A. T. Paxton, Phys. Rev. B **40**, 3616 (1989).
[25] N. D. Mermin, Phys. Rev. **137**, A1441 (1965).
[26] R. M. Wentzcovitch, J. L. Martins, and P. B. Allen, Phys. Rev. B **45**, 11372 (1992).
[27] S. Baroni, P. Giannozzi, and A. Testa, Phys. Rev. Lett. **58**, 1861 (1987).
[28] S. Baroni, A. Dal Corso, S. de Gironcoli, P. Giannozzi, C. Cavazzoni, G. Ballabio, S. Scandolo, G. Chiarotti, P. Focher, A. Pasquarello, K. Laasonen, A. Trave, R. Car, N. Marzari, and A. Kokalj (http://www.pwscf.org/).
[29] F. Birch, Phys. Rev. **71**, 809 (1947).
[30] P. Vinet, J. R. Smith, J. Ferrante, and J. H. Rose, Phys. Rev. B **35**, 1945 (1987).
[31] R. E. Cohen, O. Gülseren, and R. J. Hemley, Am. Mineral. **85**, 338 (2000).
[32] T. Tsuchiya and K. Kawamura, Phys. Rev. B **66**, 094115 (2002).
[33] T. Tsuchiya, J. Geophys. Res. **108**, 2462 (2003).
[34] Y. Wang, R. Ahuja, and B. Johansson, J. Appl. Phys. **92**, 6616 (2002).
[35] C. Bercegeay and S. Bernard, Phys. Rev. B **72**, 214101 (2005).
[36] A. D. Chijioke, W. J. Nellis, and I. F. Silvera, J. Appl. Phys. **98**, 073526 (2005).
[37] P. I. Dorogokupets and A. R. Oganov, Phys. Rev. B **75**, 024115 (2007).
[38] A. Dewaele (private communication).
[39] P. I. Dorogokupets and A. Dewaele, High Press. Res. **27**, 431 (2007).
[40] This Troullier-Martins (TM) pseudopotential is constructed from $5d^9 6s^{0.95} 6p^{0.05}$ atomic configuration. The cut-off radius of 6*s* is 2.6 a.u., which is probably too large. The HGH pseudopotential is constructed from $5s^2 5d^6 5d^{10}$ and does not have this problem.
[41] A. Dal Corso and A. Mosca Conte, Phys. Rev. B **71**, 115106 (2005).
[42] A. Kavner and R. Jeanloz, J. Appl. Phys. **83**, 7553 (1998).
[43] R. A. Cowley, Rep. Prog. Phys. **31**, 123 (1968).
[44] P. B. Allen and J. C. K. Hui, Z. Phys. B **37**, 33 (1980).
[45] J. Xie, S. de Gironcoli, S. Baroni, and M. Scheffler, Phys. Rev. B **59**, 965 (1999).
[46] S. Narasimhan and S. de Gironcoli, Phys. Rev. B **65**, 064302 (2002).
[47] R. K. Kirby, Int. J. Thermophys. **12**, 679 (1991).
[48] J. W. Arblaster, Platinum Met. Rev. **38**, 119 (1994).
[49] S. M. Collard and R. B. McLellan, Acta Metall. Mater. **40**, 699 (1992).